

# Reachability-based Identification, Analysis, and Control Synthesis of Robot Systems

Stefan B. Liu, Bastian Schürmann, and Matthias Althoff

**Abstract**—We introduce reachability analysis for the formal examination of robots. We propose a novel identification method, which preserves reachset conformance of linear systems. We additionally propose a simultaneous identification and control synthesis scheme to obtain optimal controllers with formal guarantees. In a case study, we examine the effectiveness of using reachability analysis to synthesize a state-feedback controller, a velocity observer, and an output feedback controller.

**Index Terms**—formal methods, model identification, reachability analysis

## I. INTRODUCTION

### A. Motivation

- Formal methods are mathematical techniques for reasoning about systems, their requirements, and their guarantees [1].
- Formal synthesis are frameworks where tasks are specified in precise language and automatically transform them into correct-by-construction robot controllers.

### B. Statement of contributions

In the following, we list the contributions of this work:

- We formulate a unified optimal control framework for reachability-based model identification, controller synthesis, and the combination of both.
- We propose a model identification method for non-deterministic systems, which preserves reachset conformance with respect to the test data of the real system. Computationally efficient solutions for continuous-time and discrete-time linear systems are presented using zonotopes as set representation.
- We extend reachability-based controller synthesis to general linear controller systems. Using our unified framework, we combine controller synthesis with model identification and propose an iterative method to generate optimal controller with formal guarantees for real systems.
- We extensively study the application of reachability-based methods to feedback-linearizing tracking controllers of robots. We use our approaches to obtain formal guarantees on the tracking error, velocity estimation error, and whether input constraints can be met.
- We provide software in the form of a reachability-based identification toolbox written in MATLAB. The underlying foundation is the COntinuous Reachability Analyzer (CORA) [2].

S. B. Liu and M. Althoff are with the Department of Informatics, Technical University of Munich, Garching, 85748, Germany. Email: [stefan.liu; althoff]@tum.de. B. Schürmann is Siemens AG. Email: andrea.giusti@fraunhofer.it.

Manuscript received April XX, XXXX; revised August XX, XXXX.

### C. Literature overview

Traditionally, system identification and model-based control design for continuous dynamical systems have been regarded as two separate disciplines [3]: a nominal model of a robot is identified based on an optimality criterion, e.g., minimizing a least-squares error [4], [5]; control design and stability analysis are then applied assuming that the model is an exact representation of the physical dynamics [6].

With the advance of robust control, it became clear that determining an exact model of physical systems might be unfeasible, and that instead, uncertainties should be included in the control design [7]. Such uncertainties can be additive, multiplicative [3], or parametric [8], [9]. The main criterium for the identification of such uncertainties has been their size. However, small model errors do not necessarily lead to good robust control, and large model errors do not necessarily lead to bad control performance, as [10] points out. Therein lies the motivation for *identification for control*, in which the model uncertainties are determined in a way, such that it is optimal for the control goal [3].

Model errors can be mainly divided in two ways: stochastic bounds vs. set bounds, and frequency-domain vs. time domain uncertainties. A discussion on frequency-domain uncertainties for robust control can be found in [11]. Stochastic aspects of model errors are treated in large detail in [5]. In [12], the stochastic uncertainty of the parameters of robot kinematics is identified through Monte-Carlo sampling.

In the following paragraphs, we will focus on set bounds for time domain uncertainties. Most of the previous literature belong to set-membership identification [9], [13]–[16], which usually refers to works based on finding a feasible solution set (FSS). Given an unknown model and a set of measurements, it is the goal to identify a FSS that is consistent with all measurements of the system. The general technique [13] is to model measurements, including their a priori assumed errors, as strips in parameter space. The FSS is then the intersection of all strips, such that the unknown parameter is guaranteed to be inside. It is important here to distinguish that the FSS does not actually represent non-deterministic parameters, rather it seeks to find the ‘true’ deterministic parameter value by narrowing the FSS down as much as possible. The non-determinism, in fact, must be assumed a priori. E.g., in [17], the non-deterministic disturbance of a linear system must be known a priori to identify the FSS of the system matrix parameters. As [9] showed on real robot manipulators, the set-membership identification technique frequently returns empty FSS, such that a priori non-determinisms actually have to be manually increased. Also, the authors exclude data considered as ‘out-

liers', if the measurement strip is far away from the FSS. The work in [18] proposes to use the outliers for fault detection of robots. The work in [16] presents an set-membership approach that aims to track time-varying parameters. In contrast to these works, we are interested in identifying bounds of time-varying and non-deterministic parameters, for which the mentioned FSS approaches are not suitable.

Since formal methods are increasingly applied to robotic systems, the question arises, how far verification results obtained for a model are actually transferable to the real system. This problem is also known as *model conformance* and has been treated in-depth in [19]. Most literature on set-based identification are based on the *simulation relation*, since it allows a transfer of, e.g., temporal logic properties for the entire state space. The model can be a coarse-grained abstraction of the state-space into a discrete automaton (e.g, for the navigation of mobile robots [1]), or differential equations [20], [21] with non-deterministic disturbance. Chen et al. [20] identify a linear system with non-determinism such that all state measurements are within a polytopic reachable set. Saddradini and Belta [21] identify piece-wise affine models using Mixed-Integer Linear Programming, also establishing a simulation relation between measured states with hyperrectangular reachable sets.

However, if a system is high-dimensional, but only few outputs are relevant for verification, then the simulation relation can be too restrictive and conservative. Thus, *trace* and *reachset conformance* have been proposed to relax the formal relation only to the output of a system [19]. In [22], the authors apply trace conformance by reconstructing disturbance traces for a real autonomous vehicle. The set of non-deterministic disturbances is then taken as the outer bounds of all disturbance traces. *Reachset conformance*, on the other hand, is a further relaxation which only requires that the output traces of a system must be within the reachable set of the model, instead of traces. The main advantage is that a user can now more freely choose the internal structure, as long as the output is conformant, resulting in a more flexible model-order reduction [23], or even applying black-box identification methods [24]. Although the amount of transferable properties reduces to reachability-based ones only, it is only a supposed disadvantage: many verification problems in formal methods are actually based on reachability, such as the computation of control invariant sets [25] and verifying collision avoidance [26]. First works on the identification of robot manipulators based on reachset conformance can be found in [27], [28].

A different view on set-based identification is to formulate it as a synthesis problem. The authors in [29], [30] are able to incorporate additional model knowledge as Temporal logic constraints to improve identification.

Formal controller synthesis is a large research area with many recent results in robotics, see e.g. [1] for an overview. The idea is to compute a controller which formally guarantees the satisfaction of (complex) constraints. A large area of formal controllers are abstraction based controllers [31]–[41] which satisfy complex specifications such as temporal logic expressions. By discretizing the state and input space, they obtain a finite state abstraction of the system and use techniques from automata theory to obtain controllers for the

abstracted system. The necessity to discretize the states leads to an exponential computational complexity which restricts the application to higher-dimensional systems. Some works try to avoid this problem by not abstracting the whole state space, see for example [42]–[44].

Instead of abstracting the whole state space, other approaches compute safe motion primitives, i.e., short trajectory pieces with a corresponding controller which keeps the system in a pre-defined sets. By computing many motion primitives and storing them in a maneuver automaton, they can be used with a discrete online planner, which only needs to find a suitable concatenation of motion primitives [45], [46]. There exist different methods to compute these motion primitives, for example using linear quadratic regulator (LQR) trees [47], [48] or by combining optimization with reachability analysis [49]–[51].

A well-known area of controllers which ensure the satisfaction of state and input constraints despite the presence of disturbances is robust model predictive control (MPC). In the most common implementation of tube-based MPC, an optimization algorithm iteratively optimizes a reference trajectory over a moving horizon, while a feedback controller keeps the system in a tube around the reference trajectory. For linear systems, the computation of reference trajectory and the control invariant set of the tube can be decoupled due to the superposition principle [52]–[55], while for nonlinear systems this becomes more complex. Still, there exist a number of approaches for nonlinear systems, e.g., [56]–[59].

Other ways to ensure the satisfaction of constraints are for example using an additional invariance controller [60], [61] or using control barrier functions [62], [63].

At last, we make the connection of this work to the area of robust control for robots. The approach of this paper can be directly applied for the reachability analysis of feedback-linearizing robust linear controllers, where—similarly to our work—an uncertainty of the linear system due to an imperfect model is assumed [64]. Robustness analysis involves bounding of uncertain parameters of the model, e.g., in [65, Section 8.5.3] the mass matrix and other nonlinear terms of the robot dynamics are bounded to prove uniform boundedness of the tracking error. The approach in [66] discusses a control scheme for robots, that achieves a desired tracking performance with a specified convergence rate. Uniform ultimate boundedness despite system uncertainties of the computed torque controller (which we analyse in our work) has already been shown in previous work [67]. Further works on robust control for robots are surveyed in [64].  $\mathcal{H}_\infty$ -synthesis (e.g., in [68], [69]) generate controllers that minimize the influence of disturbances on the system dynamics expressed in frequency domain. Often, such as in [69], the validation of these approaches are done in time-domain through a Monte-Carlo simulation of the uncertain parameters to analyse the systems reachability. In contrast, our work computes the reachable set directly to evaluate control performance. In fact, reachability analysis can be interpreted as a direct evaluation of robust properties such as uniform ultimate boundedness.

#### D. Structure of this paper

In Sec. II we introduce zonotopes and reachability analysis of linear systems. The reachability-based methods are presented in Sec. III. We then address the application of these methods to the tracking control problem of robot systems in Sec. IV. This paper concludes in Sec. V.

## II. PRELIMINARIES

### A. Zonotopes

The advantage of zonotopes as a set-representation is that they scale well to high dimensions. In addition, algebraic operations are closed-form, i.e., the result of an operation involving zonotopes is again a zonotope. In the following definitions, we define its generator-space and halfspace representation, as well as the algebraic operations. We denote sets in calligraphic letters (e.g.,  $\mathcal{A}$ ), matrices with upper case letters (e.g.,  $A$ ), vectors by  $\vec{v}$ , and scalar values by lower case letters (e.g.,  $a$ ). The  $n$ -dimensional identity matrix is denoted by  $I_n$ .

**Definition 1** (Zonotope: generator-space representation [70]). *A zonotope  $\mathcal{Z}$  is defined by a center  $\vec{c}$ ; a generator matrix  $G$ , where  $\alpha^{(h)}\vec{g}^{(h)}$  is its  $h$ -th column; and  $\alpha^{(h)} > 0$ , which is a scaling factor determining the length of each generator:*

$$\begin{aligned} \mathcal{Z} = (\vec{c}, G) &:= \left\{ \vec{x} = \vec{c} + \sum_{h=1}^p \beta_h \vec{g}^{(h)} \middle| \beta_h \in [-\alpha^{(h)}, \alpha^{(h)}] \right\}. \\ &= \left\{ \vec{x} = \vec{c} + \sum_{h=1}^p \beta \alpha^{(h)} \vec{g}^{(h)} \middle| \beta \in [-1, 1] \right\} = (\vec{c}, G' \operatorname{diag}(\alpha)). \end{aligned}$$

**Definition 2** (Zonotope: halfspace representation [70]). *A zonotope  $(\vec{c}, G)$  with  $p$  generators has  $2\binom{p}{n-1}$  facets. The generators that span a facet are obtained by cancelling  $p-n+1$  generators from the  $G$ -matrix. This is denoted by  $G^{(\gamma, \dots, \eta)}$ , where  $\gamma, \dots, \eta$  are the  $p-n+1$  indices of the generators that are taken out of  $G$ . The halfspace representation of a zonotope is  $N \cdot \vec{x} \leq \vec{d}$ , where*

$$N = \begin{bmatrix} N^+ \\ -N^+ \end{bmatrix}, \quad \vec{d} = \begin{bmatrix} \vec{d}^+ \\ \vec{d}^- \end{bmatrix},$$

and the  $j$ -th row  $j \in 1..(\binom{p}{n-1})$  of  $N^+$ ,  $\vec{d}^+$ , and  $\vec{d}^-$  are:

$$\begin{aligned} \vec{n}_j^+ &:= \operatorname{nX}(G^{(\gamma, \dots, \eta)}) / \|\operatorname{nX}(G^{(\gamma, \dots, \eta)})\|_2 \\ \vec{d}_j^+ &:= \vec{n}_j^{+T} \cdot \vec{c} + \Delta d_j \\ \vec{d}_j^- &:= -\vec{n}_j^{+T} \cdot \vec{c} + \Delta d_j \\ \Delta d_j &:= \sum_{\nu=1}^p |\vec{n}_j^{+T} \cdot \vec{g}^{(\nu)}| \\ \operatorname{nX}(H) &:= [\dots, (-1)^{j+1} \det(H^{[j]}), \dots]^T. \end{aligned}$$

**Definition 3** (Minkowski sum of zonotopes). *The Minkowski sum of sets is defined as  $\mathcal{A} \oplus \mathcal{B} = \{\vec{a} + \vec{b} \mid \vec{a} \in \mathcal{A}, \vec{b} \in \mathcal{B}\}$ . For zonotopes, their Minkowski sum has a closed-form solution in generator space*

$$\mathcal{Z}_1 \oplus \mathcal{Z}_2 = (\vec{c}_1, G_1) \oplus (\vec{c}_2, G_2) = (\vec{c}_1 + \vec{c}_2, [G_1, G_2]).$$

**Definition 4** (Linear transformation of zonotopes). *Zonotopes are closed under linear transformation:  $A\mathcal{Z} = (A\vec{c}, AG)$ .*

**Definition 5** (Interval hull of zonotopes). *The interval hull  $\mathcal{I}(\mathcal{Z}) = \{\vec{i}^-, \vec{i}^+\}$  is a tight outer-approximation of a zonotope  $\mathcal{Z} = (\vec{c}, [\dots, \vec{g}^{(h)}, \dots])$ , which is defined by*

$$\vec{i}^- := \vec{c} - \delta \vec{g}, \quad \vec{i}^+ := \vec{c} + \delta \vec{g}, \quad \delta \vec{g} := \sum_{h=1}^p |\vec{g}^{(h)}|.$$

**Definition 6** (Norm of zonotopes). *We define the norm of a zonotope as sum of the side lengths of its interval hull:  $\|\mathcal{Z}\| := \|\delta \vec{g}\|_1$ , where  $\|\cdot\|_1$  is the (scalar) 1-norm.*

### B. Reachability analysis of linear time-invariant systems

This paper mainly regards linear systems  $S$  with uncertainties described by the following differential inclusion

$$\begin{aligned} \dot{\vec{x}}(t) &\in A\vec{x}(t) + B\vec{u}(t) \oplus \mathcal{W}, \\ \vec{y}(t) &\in C\vec{x}(t) + D\vec{u}(t) \oplus \mathcal{V} \end{aligned} \quad (1)$$

If input  $\vec{u}(t)$  and the uncertainties  $\mathcal{V}, \mathcal{W}$  are constant within one sampling time  $\Delta t$ , then we can formulate a discrete-time version  $\tilde{S}$ , where the integer  $k = t/\Delta t$ :

$$\begin{aligned} \vec{x}[k+1] &\in \tilde{A}\vec{x}[k] + \tilde{B}\vec{u}[k] \oplus \tilde{E}\mathcal{W}, \\ \vec{y}[k] &\in C\vec{x}[k] + D\vec{u}[k] \oplus \mathcal{V}, \end{aligned} \quad (2)$$

where the system matrices are

$$\begin{aligned} \tilde{A} &= e^{At_s}, \quad \tilde{B} = \int_0^{\Delta t} e^{A(t-\tau)} B d\tau \\ \tilde{E} &= \int_0^{\Delta t} e^{A(t-\tau)} E d\tau \end{aligned}$$

The *reachable set*  $\mathcal{R}$  of a linear system  $\tilde{S}$  after one time-step is computed through a set-based evaluation of (2):

$$\begin{aligned} \mathcal{R}[k+1] &= C\tilde{A}\mathcal{X}[k] \oplus C\tilde{B}\vec{u}[k] \\ &\quad \oplus C\tilde{E}\mathcal{W} \oplus D\vec{u}[k] \oplus \mathcal{V}, \end{aligned} \quad (3)$$

where  $\mathcal{X}[k]$  is the current set of states. If an initial state  $x[0]$  is given, then the reachable set at  $k$  can be computed by recursively applying (3):

$$\begin{aligned} \mathcal{R}[k] &= C\tilde{A}^k x[0] \oplus \sum_{i=0}^{k-1} C\tilde{A}^i \tilde{B}\vec{u}[i] \\ &\quad \oplus \bigoplus_{i=0}^{k-1} C\tilde{A}^i \tilde{E}\mathcal{W} \oplus D\vec{u}[k] \oplus \mathcal{V}. \end{aligned} \quad (4)$$

Since (4) only involves the Minkowski sum and linear transformations, the resulting reachable set is closed-form and exact for linear systems  $\tilde{S}$ . It is an inner-approximation of the reachable sets of linear systems  $S$ , as shown by the following Lemma

**Lemma 1.** *By moving the set  $\mathcal{W}$  out of the convolution integral of the particular solution of a linear time-invariant system, assuming  $w$  is constant, the result is an inner-approximation of the time-varying  $w(\tau)$  case.*

$$\begin{aligned} \left\{ \int_0^t e^{A(t-\tau)} d\tau w \mid w \in \mathcal{W} \right\} &\subseteq \\ \left\{ \int_0^t e^{A(t-\tau)} w(\tau) d\tau \mid \forall \tau : w(\tau) \in \mathcal{W} \right\}. \end{aligned}$$

The notation already shows that the right-hand side contains more solutions than the left-hand side.  $\square$

For nonlinear systems in the form of  $\dot{x} \in f(x, u, \mathcal{W})$ , the solution is generally non-closed. Further works on outer and inner-approximations of reachable sets are surveyed in [71].

In this work, we regard the compositional analysis of linear subsystems. We define the operators  $\text{series}(S_1, S_2)$  and  $\text{feedback}(S_1, S_2)$ , which refer to the series and feedback interconnection of linear multi-input, multi-output subsystems  $S_1$  and  $S_2$ , for which the results are also linear systems. The derivation is straight-forward and details can be found in the supplied software code and in [72].

### III. REACHABILITY-BASED METHODS

This section describes the theoretical contribution, which is our methodology for reachability-based identification and control. These methods share a common optimization framework, which we introduce in Sec. III-A. We subsequently derive reachset conformant model identification in Sec. III-B, reachability-based control synthesis in Sec. III-C, and the combination of both in Sec. III-D.

#### A. Reachability-based optimization framework

In our previous work [51], we showed how we can obtain a safe controller by optimizing over the reachable sets of the closed-loop dynamics. We extend this idea to more general system structures. As we will see, all problems at hand, i.e., reachset conformant identification, controller synthesis, and the combination of both, can be solved by optimizing over reachable sets. To do so, we consider the interconnected system, e.g., the closed-loop system resulting from the plant in combination with the controller, and compute its reachable sets  $\mathcal{R}$ . In all cases, we obtain a linear system with variable parameters, e.g., unknown model or controller parameters. Donating this parameter set as  $\mathcal{P}$ , the optimization problem in its general form can be written as

$$\min_{\mathcal{P}} \quad \text{cost}(\mathcal{R}), \quad (5a)$$

$$\text{subject to} \quad \text{constraints}(\mathcal{R}). \quad (5b)$$

The cost and constraints functions both depend on the reachable set or projections of the reachable set on subspaces and are going to be defined in detail in the following subsections. Depending on the type of parameters, the cost and constraint functions might become nonlinear and nonconvex. In this case we can use nonlinear programming to obtain optimal parameters. Overall, we solve all problems at hand with the same set of optimization techniques, while the incorporation of reachability analysis in the synthesis provides formal guarantees and ensures constraint satisfaction despite the presence of disturbances and uncertain measurements.

#### B. Reachset conformant model identification

Verifying reachability-based properties of a robot requires a reachset conformant model. We apply the definition of [19] to measureable physical systems:

**Definition 7** (Reachset conformance). *Given is a physical system and its model. From the physical system, we perform a series of test cases, where the  $m$ -th case consists of the input  $u_m(t)$ , an initial state  $x(0)$ , and the measured output  $y_m(t)$ , where  $t \in [0, t^*]$ . From the model, we compute the reachable set  $\mathcal{R}^{(m)}(t)$  for each  $u_m(t)$  and  $x(0)$ . The model is reachset conformant in the time interval  $[0, t^*]$ , iff*

$$\forall m : \forall t \in [0, t^*] : y_m(t) \subseteq \mathcal{R}^{(m)}(t),$$

which is a set inclusion problem.

The task of model identification is thus to get an optimal set of model parameters  $\mathcal{P}$ , such that reachset conformance is preserved. For the general open-loop identification problem, we propose to minimize the norm of the reachable set integrated over  $t \in [0, t^*]$  and over all test cases  $m$ :

$$\min_{\mathcal{P}} \quad \sum_m \int_0^{t^*} \|\mathcal{R}^{(m)}(t)\| dt, \quad (6a)$$

$$\text{subject to} \quad \forall m : \forall t : y_m(t) \subseteq \mathcal{R}^{(m)}(t). \quad (6b)$$

This general formulation is applicable to nonlinear systems. For the remainder if this subsection, we derive a version for linear systems with  $\mathcal{P} = \{A, B, C, D, E, F, \mathcal{V}, \mathcal{W}\}$ , that is much more computationally efficient to solve. At first, we show that we can remove the the sum  $\sum_m$  and the quantifier  $\forall m$  for linear systems by using the superposition principle. We subtract the nominal output solution

$$y_m^*[k] := C \left( \tilde{A}^k x[0] + \sum_{i=0}^{k-1} \tilde{A}^i \tilde{B} u_m[i] \right) + D u_m[k], \quad (7)$$

which is (2) excluding the non-deterministic parameters, from the reachable set defined in (3):

$$\mathcal{R}_a[k] := \mathcal{R}^{(m)}[k] - y_m^*[k] = \bigoplus_{i=0}^{k-1} \bar{E}_i \mathcal{W} \oplus F \mathcal{V},$$

where  $\bar{E}_i = C \tilde{A}^i \tilde{E}$ . We define the non-deterministic parameters as zonotopes  $\mathcal{V} := (\vec{c}_V, G_V)$  and  $\mathcal{W} := (\vec{c}_W, G_W)$ , such that  $\mathcal{R}_a[k]$  has a closed-form solution:

$$\mathcal{R}_a[k] = (\vec{c}_k, G_k), \quad \vec{c}_k := \left[ \sum_{i=0}^{k-1} \bar{E}_i \quad F \right] \begin{bmatrix} \vec{c}_W \\ \vec{c}_V \end{bmatrix}, \quad (8)$$

$$G_k := [\bar{E}_0 G_W \quad \dots \quad \bar{E}_{k-1} G_W \quad F G_V]. \quad (9)$$

When applying Def. 6, we immediately see that the zonotope norm  $\|\mathcal{R}_a[k]\| = \|\mathcal{R}^{(m)}(t)\|$ , and is independent from  $m$  for linear systems.

Also using the superposition principle, we subtract  $y_m^*[k]$  from the measurement  $y_m[k]$ , such that for each test case,  $y_{a,m}[k] := y_m[k] - y_m^*[k]$  and the following holds for linear systems:

$$\begin{aligned} \forall m : \forall k : y_m[k] \subseteq \mathcal{R}^{(m)}[k] \\ \iff \forall m : \forall k : y_{a,m}[k] \subseteq \mathcal{R}_a[k] \\ \iff \forall k : \bigcup_m y_{a,m}[k] \subseteq \mathcal{R}_a[k]. \end{aligned}$$

Thus, we formulate the open-loop identification problem for linear systems

$$\min_{A,B,C,D,E,F,\mathcal{V},\mathcal{W}} \quad \|\mathcal{R}_a(t)\|dt, \quad (10a)$$

$$\text{subject to} \quad \forall k : \bigcup_m y_{a,m}[k] \subseteq \mathcal{R}_a[k]. \quad (10b)$$

The following two Lemmas present the cost and constraint function for the above optimization problem, which then result into Theorem 1 and 2.

**Lemma 2.** *The cost (10a) for the identification of linear systems is linear in the scaling parameters  $\alpha_W$  and  $\alpha_V$  of the zonotopic non-determinisms  $\mathcal{W}, \mathcal{V}$ :*

$$\int_0^{t^*} \|\mathcal{R}(t)\|dt = \vec{\gamma} \begin{bmatrix} \alpha_W \\ \alpha_V \end{bmatrix} \quad (11)$$

$$\gamma := \vec{1}^T \left[ \sum_{k=0}^a \left| \sum_{i=0}^{k-1} t_s \bar{E}_i G'_W \right|, \quad |FG'_V| \right], \quad (12)$$

where  $\vec{1}$  is a vector full of ones and  $a = t^*/\Delta t$ . Please be reminded, that we use the notation  $G := G' \text{diag } \alpha$  here (see Def. 1).

*Proof.* To compute the norm (see Def. 6), we only require the generators of  $\mathcal{R}[k]$ . Thus, for discrete-time linear systems,  $\int_0^{t^*} \|\mathcal{R}(t)\|dt = \sum_k t_s \|\mathcal{R}_a[k]\|$ . Each side length of  $\mathcal{I}(\mathcal{R}_a[k])$  according to Def. 5 is

$$\begin{aligned} \vec{\delta}g_k &= \left| \begin{bmatrix} \bar{E}_0 G_W & \dots & \bar{E}_{k-1} G_W & FG_V \end{bmatrix} \right| \vec{1} \\ &= \left| \begin{bmatrix} \bar{E}_0 G'_W & \dots & \bar{E}_{k-1} G'_W & FG'_V \end{bmatrix} \right| \begin{bmatrix} \alpha_W \\ \dots \\ \alpha_W \\ \alpha_V \end{bmatrix} \\ &= \left| \left[ \sum_{i=0}^{k-1} \bar{E}_i G'_W \quad FG'_V \right] \right| \begin{bmatrix} \alpha_W \\ \alpha_V \end{bmatrix}. \end{aligned}$$

With  $\|\vec{\delta}g_i\|_1 := \vec{1}^T \vec{\delta}g_i$ , we obtain  $\vec{\gamma} \begin{bmatrix} \alpha_W \\ \alpha_V \end{bmatrix}$  by evaluating  $\sum_k t_s \|\mathcal{R}_a[k]\| = \sum_k t_s \vec{1}^T \vec{\delta}g_i$ .  $\square$

**Lemma 3.** *The constraint (10b) for the identification of linear systems is linear in  $\vec{\xi} = [\vec{c}_W, \vec{c}_V, \vec{\alpha}_W, \vec{\alpha}_V]^T$ , if we use the halfspace representation of  $\mathcal{R}_a[k]$ :*

$$\forall k \in \left[ 0, \frac{t_e}{t_s} \right] : \forall m : N_k y_{a,m}[k] \leq D_k \vec{\xi}, \quad (13)$$

where the  $j$ -th row of  $N_k$  and  $D_k$  are the facets of the zonotope  $\mathcal{R}_a[k]$ , s.t.

$$\vec{n}_{j,k} = \text{nX}(G'_k \langle \gamma, \dots, \eta \rangle)^T / \|\text{nX}(G'_k \langle \gamma, \dots, \eta \rangle)\|_2. \quad (14)$$

$$\begin{aligned} \vec{d}_{j,k}^+ &= \left[ \sum_{i=0}^{k-1} \vec{n}_{j,k}^+ \bar{E}_i \quad \vec{n}_{j,k}^+ F \right. \\ &\quad \left. \sum_{i=0}^{k-1} |\vec{n}_{j,k}^+ \bar{E}_i G'_W| \quad |\vec{n}_{j,k}^+ FG'_V| \right]. \end{aligned} \quad (15)$$

$$\begin{aligned} \vec{d}_{j,k}^- &= \left[ -\sum_{i=0}^{k-1} \vec{n}_{j,k}^+ \bar{E}_i \quad -\vec{n}_{j,k}^+ F \right. \\ &\quad \left. \sum_{i=0}^{k-1} |\vec{n}_{j,k}^+ \bar{E}_i G'_W| \quad |\vec{n}_{j,k}^+ FG'_V| \right]. \end{aligned} \quad (16)$$

*Proof.* Consider the halfspace representation of a zonotope  $\mathcal{R}_a[k] = (\vec{c}_k, G_k)$  using the Def. 2. We show that  $\vec{n}_{j,k}^+$  is independent from  $\vec{\alpha}$  for any generator matrix:

$$\begin{aligned} \text{nX}(G' \text{diag}(\vec{\alpha})) &= \\ &= [\dots, (-1)^{i+1} \det(G'^{[i]} \text{diag}(\vec{\alpha})), \dots]^T, \\ &= \det(\text{diag}(\vec{\alpha}))[\dots, (-1)^{i+1} \det(G'^{[i]}), \dots]^T, \\ &= \left( \prod \vec{\alpha} \right) \cdot \text{nX}(G'), \end{aligned}$$

and since  $\prod \vec{\alpha}$  is a positive scalar, the two-norm

$$\left\| \left( \prod \vec{\alpha} \right) \cdot \text{nX}(G') \right\|_2 = \left( \prod \vec{\alpha} \right) \|\text{nX}(G')\|_2,$$

such that  $\vec{\alpha}$  completely cancels out. To obtain  $D_k$  we apply the definition of  $\mathcal{R}_a[k]$  in (8). From  $\Delta d_{j,k}$ , we extract  $\alpha_W, \alpha_V$  in a similar way as in the proof of Lemma 2:

$$\Delta d_{j,k} = \left[ \sum_{i=0}^{k-1} |\vec{n}_{j,k}^+ \bar{E}_i G'_W| \quad |\vec{n}_{j,k}^+ FG'_V| \right] \begin{bmatrix} \alpha_W \\ \alpha_V \end{bmatrix}. \quad (17)$$

$\square$

The following two theorems formulate the reachset conformant identification problem (10a) and (10b) for linear systems.

**Theorem 1** (Reachset conformant identification of additive non-deterministic parameters of linear systems). *Given a linear system (1), where  $\mathcal{V}$  and  $\mathcal{W}$  are zonotopes, the reachset conformant identification problem is a linear program, where  $\mathcal{P} = \{\vec{c}_W, \vec{c}_V, \vec{\alpha}_W, \vec{\alpha}_V\}$  are the model parameters to be identified, (11) is the cost, and (13) are the constraints.*

*Proof.* Check proofs of Lemma 2 and 3. Given  $\mathcal{P}$ , both cost (11) and the constraint function (13) are linear.  $\square$

**Theorem 2** (Reachset conformant identification of linear systems). *Given a linear system (1), where  $\mathcal{V}$  and  $\mathcal{W}$  are zonotopes, the reachset conformant identification problem is generally a nonlinear program, where  $\mathcal{P} = \{A, B, C, D, E, F, \mathcal{V}, \mathcal{W}\}$  are the variables to be identified, (11) is the cost, and (13) are the constraints.*

*Proof.* Check proofs of Lemma 2 and 3.  $\square$

**Remark 1.** *We provide some remarks on the implementation of the above theorems:*

- Theorem 2 can be approached in a cascading way: an inner layer solves for  $\{\vec{c}_W, \vec{c}_V, \vec{\alpha}_W, \vec{\alpha}_V\}$  using linear programming (Theorem 1), while the outer layer solves for  $\{A, B, C, D, E, F, G'_W, G'_V\}$  through nonlinear programming. An MATLAB implementation is provided together with this paper.
- The solution space can also be reduced by estimating  $\{A, B, C, D\}$  using the subspace method based on least-squares optimization [5, Chapter 4.3], although [20] has shown that such an approach is generally not optimal.
- To compute  $y^*[k]$ , an estimation of the initial state  $x[0]$  is required, similar to other identification algorithms (e.g., subspace methods in [5]).

The influence of non-determinism on the linear system (1) is modelled by the matrices  $E$  and  $F$ . The main motivation behind it is that, for systems with high-dimensional state spaces,

engineering knowledge can be applied to accurately determine where non-determinism appears, and therefore reducing the number of optimization parameters. The following Lemma evaluates, whether  $E$  and  $F$  have been chosen correctly.

**Lemma 4.** *A linear system with variable  $\mathcal{W}, \mathcal{V}$  can capture all non-determinisms of the system, if*

$$\forall k : \quad J_k = [C\bar{E}_0, \dots, C\bar{E}_{k-1}, F], \quad (18)$$

has full (row) rank. If it is not full for some  $k$ , then the signals  $\vec{y}_a[k]$  must only appear in  $S(J_k)$ , which is the linear subspace of  $J_k$ .

*Proof.* If  $J_k$  has full rank, then matrix  $J_k : \{\mathcal{W}, \mathcal{V}\} \rightarrow y[k]$  is in (3) is a surjective function (cite). When not full rank, then it is only surjective with respect to the image  $S(J_k)$ .  $\square$

**Remark 2.** *To check, if  $\forall k : \vec{y}_a[k] \in S(J_k)$ , we can simply evaluate whether  $\vec{y}_a[k] = J_k J_k^+ \vec{y}_a[k]$  is satisfied, where  $(\cdot)^+$  is the Moore-Penrose inverse operator [73].*

A thought experiment demonstrates the use of the above Lemma: the initial state  $x[0]$ , which is required for reachability analysis, is usually not measurable and can only be estimated with an estimation error  $\mathcal{X}_0$ , that has not been explicitly modelled in our linear system (2). However, if the conditions Lemma 4 is fulfilled, then  $\mathcal{X}_0$  is remapped onto  $\mathcal{W}$  and  $\mathcal{V}$ . After one time-step,

$$\mathcal{W} \times \mathcal{V} = J_1^+ J_1 (\mathcal{W}^* \times \mathcal{V}^*) \oplus J_1^+ C \tilde{A} \mathcal{X}_0 \quad (19)$$

is a possible solution of the remap. An interesting side result of this example is that it allows us to evaluate the performance of state estimation algorithms: higher-performing state estimation results in a decreasing  $\mathcal{X}_0$ , which strictly decreases the size of identified  $\mathcal{W} \times \mathcal{V}$ , as shown in (19).

An additional note for extensions to nonlinear systems: since reachability algorithms of nonlinear systems are generally non-closed, strict reachset conformance as defined in Def. 7 requires an inner-approximation of reachable sets.

### C. Reachability-based controller synthesis

We consider a linear time-invariant controller system

$$\begin{aligned} \dot{\vec{x}}_c(t) &= A_c \vec{x}_c(t) + B_c \vec{u}_c(t), \\ \vec{y}_c(t) &= C_c \vec{x}_c(t) + D_c \vec{u}_c(t), \end{aligned} \quad (20)$$

with subscript  $c$ . We denote the plant with subscript  $p$  and the closed-loop linear system with subscript  $z$  (see Fig. 1). State  $\vec{x}_c$  describes the internal state of the controller, output  $\vec{y}_c$  is connected to the input of the plant, and input  $\vec{u}_c$  accepts feedback from the plant. We regard the problem of synthesizing a controller, that lets the output of the closed-loop system  $\vec{y}_z(t)$  optimally track the reference  $\vec{y}_{\text{ref}}(t)$ , while formally guaranteeing the satisfaction of state and input constraints.

To do so, we use techniques from [51], [74], where we combine the controller synthesis with reachable set computation in a single optimization problem in the form of (5a)–(5b). We use the superposition principle [51] to separate the problems of generating the reference input  $\vec{u}_{\text{ref}}(t)$ , and synthesizing the

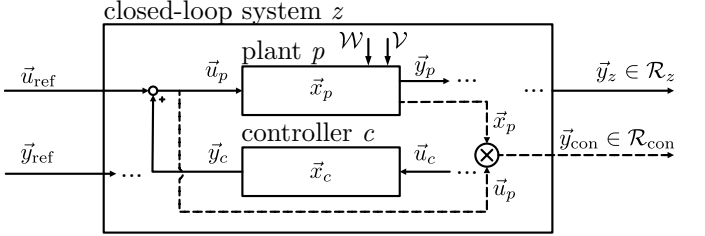


Fig. 1. Plant and controller are subsystems of the closed-loop system. The interconnection of  $\vec{y}_{\text{ref}}$ ,  $\vec{u}_c$ ,  $\vec{y}_c$ ,  $\vec{y}_z$  depends on the application.

optimal disturbance rejection provided by  $\vec{y}_c(t)$ , by defining the plant input as

$$\vec{u}_p(t) := \vec{u}_{\text{ref}}(t) + \vec{y}_c(t), \quad (21)$$

which, in turn, means that the output of the closed-loop system will be the sum of the reference and the tracking error  $\vec{y}_e(t)$ :

$$\vec{y}_z(t) = \vec{y}_{\text{ref}}(t) + \vec{y}_e(t), \quad (22)$$

In the following, we discuss our choice of parameters, constraint, and cost function.

*Parameters:* The controller is parametrized through the choice of controller matrices  $A_c, B_c, C_c$ , and  $D_c$ . Note that a fixed state feedback of the form  $\vec{u}(\vec{x}) = K\vec{x}$ , as regarded in our previous work in [51], is a special case of (20), with  $A_c = B_c = C_c = 0$ ,  $D_c = K$ , and  $C = I$  for the plant.

*Cost:* Analogously to [51], we use the norm of the final reachable set  $\|\mathcal{R}_z(t_\infty)\|$  of the closed-loop system as a cost function for the optimization problem. To obtain the final reachable set  $\mathcal{R}_z(t_\infty)$ , we compute the reachable set starting from a small initial set until it converges, i.e., it holds that  $\mathcal{R}_z(t + \Delta t) \subseteq \mathcal{R}_z(t)$ , for some  $\Delta t \geq 0$ . In this case, the reachable set converged and since we consider time-invariant systems, any future reachable sets will remain in  $\mathcal{R}_z(t)$ . By setting  $\vec{u}_{\text{ref}}(t) := 0$ , which implies  $\vec{y}_{\text{ref}}(t) = 0$ , the set  $\mathcal{R}_z(t_\infty)$  corresponds to the minimal robust positively invariant set [25] of the tracking error. Note that depending on the stability of the system and the numerical computation, this convergence might not happen; therefore, we apply a convergence tolerance criterium similar [25] to terminate the computation.

*Constraints:* We consider constraints sets  $\mathcal{U}_p$  and  $\mathcal{X}_p$  for the plant input and state by combining them into an output constraint set  $\mathcal{Y}_{\text{con}} = \mathcal{U}_p \times \mathcal{X}_p$ , and provide an output signal  $\vec{y}_{\text{con}}(t) = [\vec{u}_p(t), \vec{x}_p(t)]^T$ , such that

$$\vec{y}_{\text{con}}(t) \in \mathcal{Y}_{\text{con}}, \quad \forall t \in \mathbb{R}_0^+. \quad (23)$$

In order to ensure that the constraints are satisfied despite the decoupled synthesis of the tracking controller and reference trajectory, we divide the input constraints into two parts  $\mathcal{U}_{\text{ref}}$  and  $\mathcal{Y}_c$  for the reference trajectory and for the tracking controller, respectively. We choose these sets such that

$$\mathcal{U}_{\text{ref}} \oplus \mathcal{Y}_c \subseteq \mathcal{U}_p. \quad (24)$$

For simpler computation, we choose  $\mathcal{Y}_c$  as a polytope. Notice, that in order to analyze the reachability of  $\vec{x}_p$ , the plant model must also be reachset conformant regarding  $\vec{x}_p$ . The identification in Sec. III-B can be straight-forwardly extended

by considering  $\vec{x}_p$  as additional plant model outputs, and by extending the output measurements  $\vec{y}_m$  (see Def. 7) with an estimation of the states, e.g., through observers. However, due to the estimation errors, we introduce additional conservativeness in the identified model, as can be seen in (19). Therefore,  $\vec{y}_{\text{con}}$  should only include the elements of  $\vec{x}_p$  that are relevant for state constraints.

We formulate the resulting optimal control problem

$$\min_{A_c, B_c, C_c, D_c} \|\mathcal{R}_z(t_\infty)\|, \quad (25a)$$

$$\text{subject to} \quad \forall t : \mathcal{R}_{\text{con}}(t) \subseteq \mathcal{Y}_c. \quad (25b)$$

Since  $\mathcal{R}_z$  and  $\mathcal{R}_{\text{con}}(t)$  are zonotopes, checking the constraint (25b) requires only to check if a zonotope is inside a polytope. As shown in [74], this can be computed very efficiently.

In contrast to identification, optimizing the feedback matrix, which is multiplied with the output, cannot be expressed as a linear problem anymore. To be formally safe, we also consider time-varying disturbances when computing an over-approximative reachable set during the optimization problem, which prevents us from using under-approximations like (4), see Lemma 1. As discussed in [51], the resulting optimization problem can be solved using standard nonlinear programming techniques.

#### D. Identification for control

Given the optimization framework in Sec. III-A, the formulation of identification for control is straightforward: the control synthesis objective (25a) replaces the open-loop identification cost (10a), while the constraints (10b) and (25b), as well as the parameters  $\mathcal{P}$ , are merged. For linear systems, the optimization problem takes the form

$$\min_{\mathcal{P}} \|\mathcal{R}_z(t_\infty)\|, \quad (26a)$$

$$\text{subject to} \quad \forall k \in [0, \infty] : \forall m : N_k y_{a,m}[k] \leq D_k \vec{\xi}, \quad (26b)$$

$$\forall t : \mathcal{R}_{\text{con}}(t) \subseteq \mathcal{Y}_c, \quad (26c)$$

$$\mathcal{P} := \{A, B, C, D, E, F, \mathcal{V}, \mathcal{W}, A_c, B_c, C_c, D_c\},$$

which we solve using standard nonlinear programming algorithms. Although the formulation is straight forward, several points must be considered for the actual application:

- Constraint (26b) requires  $k$  to go to  $t_\infty/t_s$ , which can be too large, leading to a high number of linear constraints. During experiments, we discovered that one can choose a  $k_{\max} < t_\infty/t_s$ , above which the result of the control synthesis does not change anymore.
- The set of parameters  $\mathcal{P}$  is very large. In practice, we do not optimize all parameters. Rather, we make an educated selection based on engineering knowledge. In Sec. IV, we will give many hints on how such a choice might look like for robot systems.
- The chosen order (system dimension) of the plant model can be too low, such that certain dynamic behaviors of the system are not sufficiently covered.

The last point is a problem which we frequently encountered: a plant model, whose order is too low, lets the synthesis

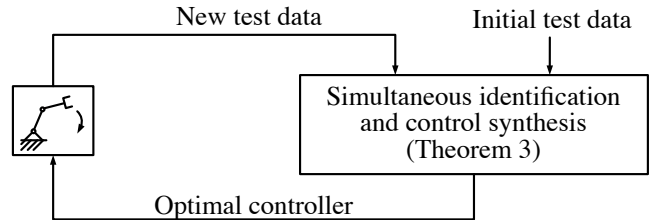


Fig. 2. Iterative procedure for simultaneous reachability-based identification and control synthesis. The iterations stops, when new test data do not lead to an updated identified model and optimal controller

algorithm optimize for a controller that would destabilize the plant. There are two reasons for this behavior: 1) the formal explanation is that a reachset conformant plant model does not transfer stability properties of a model to the real plant [19]; rather, all unknown dynamics should be reflected within non-deterministic parameters, including the ones which have been excited by the destabilization; and 2) the chosen test cases for identification (see Def. 7) do not sufficiently excite the relevant unknown dynamics.

Regarding the first reason: it is not practical to create a model that covers all dynamics of a physical system, since the synthesis task would become increasingly complex; however, dynamically relevant behavior for the application should be considered. Nonetheless, without experience, it is hard to know a priori, which dynamics is relevant. Regarding the second reason: explicitly testing unstable behavior could pose danger for the robotic hardware, as well as the operator.

To encounter these challenges, we propose an iterative synthesis procedure, which is inspired by the one proposed in [3]: instead of using one model, we propose to approach the synthesis problem with multiple model candidates with differing model orders. Infeasible model candidates will be eliminated after each iteration. From the model candidates that converge to feasible solutions, we choose the best one according to our cost criterium. The iterative process is depicted Fig. 2 and goes as follows for each model candidate:

- 1) From an initial set of test cases we solve (26).
- 2) Using this controller, we run the robot and obtain a new set of test data.
- 3) If the new test data is reachset conformant, then the control synthesis has converged. Otherwise, repeat step 1 including the new data.

## IV. A CASE STUDY ON ROBOT MANIPULATORS

We demonstrate the applicability of our newly proposed methods for robot systems by studying the reachability-based design of feedback-linearizing controllers for a 6-DOF manipulator. We use reachability analysis to compute and minimize the ultimate bounds of the tracking error. We start with investigating modelling choices for optimal identification results. We subsequently examine the application of our methods on the synthesis of a state-feedback controller, a linear velocity observer, and an output-feedback controller.

### A. Modelling choices and open-loop identification

The system at hand is a Schunk LWA-4P 6-DOF robot manipulator. Each joint has a local current controller and an encoder feedback measuring the angular joint position. A Speedgoat Real-Time Target Machine acts as a centralized controller which sends control currents over a CANopen fieldbus system, and receives the position feedback. The sampling time of the centralized controller is  $t_s = 4$  ms. The following paragraphs describe the subsystems involved in this case study.

a) *Robot dynamics*: The rigid-body model of a robot can be described by

$$M(\vec{q})\ddot{\vec{q}} + \vec{c}(\vec{q}, \dot{\vec{q}}) + \vec{g}(\vec{q}) = \vec{\tau}, \quad (27)$$

where  $\vec{q}, \dot{\vec{q}}, \ddot{\vec{q}}$  are the position, velocity, and acceleration of the robot joints,  $M$  is the mass matrix,  $\vec{c}$  are the Coriolis and centripetal forces,  $\vec{g}$  are the gravity forces, and  $\vec{\tau}$  are the joint torques. The feedback linearization technique

$$\vec{\tau} = M(\vec{q})\vec{u} + \vec{c}(\vec{q}, \dot{\vec{q}}) + \vec{g}(\vec{q}) \quad (28)$$

implements an internal control loop with a new input  $\vec{u}$ , such that the system dynamics become  $\ddot{\vec{q}} = \vec{u}$  through inserting (28) into (27). From the outside, the robot behaves like a decoupled linear system. However, the feedback linearization is usually imperfect [7]; the effects can be mitigated using disturbance observers such as [75]. Nevertheless, we consider an unknown additive disturbance  $\mathcal{W} \in \mathbb{R}^2$ , and an unknown position feedback error  $\mathcal{V} \in \mathbb{R}$ . The resulting state-space model for each joint is:

$$\begin{aligned} \dot{\vec{x}}_r &= \begin{bmatrix} 0 & 1 \\ 0 & 0 \end{bmatrix} \vec{x}_r + \begin{bmatrix} 0 \\ 1 \end{bmatrix} u_r + \mathcal{W}, \\ y_r &= \begin{bmatrix} 1 & 0 \end{bmatrix} \vec{x}_r + \mathcal{V} \end{aligned}$$

where  $\vec{x}_r = [q, \dot{q}]^T$ . The discrete-time version is obtained by applying (2).

b) *State-feedback control*: The inverse dynamics tracking controller [65, Section 8.5] is characterized by the feedback linearization in (28) and a state-feedback term for each robot joint:

$$u_r := y_c = [1 \quad k_p \quad k_d] \vec{u}_c, \quad (29)$$

where  $u_c = [\ddot{q}_d, q_d - \hat{q}, \dot{q}_d - \dot{\hat{q}}]^T$ , the values  $q_d, \dot{q}_d, \ddot{q}_d$  denote the desired trajectory, and  $\hat{q}, \dot{\hat{q}}$  are the observation of robot position and velocity. The gains  $k_p, k_d$  are designed by choosing a natural frequency  $\omega$  and the damping ratio  $\zeta$ , s.t.  $k_p := \omega^2, k_d := 2\zeta\omega$  [65].

c) *Observer*: The above controller requires a full state feedback; however, only the robot position is measurable. We thus require an online state estimation and therefore choose the linear high-gain observer from [76]. Its dynamics for each joint is

$$\dot{\vec{x}}_o = \begin{bmatrix} -h_1 & 1 \\ -h_2 & 0 \end{bmatrix} \vec{x}_o + \begin{bmatrix} h_1 \\ h_2 \end{bmatrix} u_o, \quad (30)$$

$$\vec{y}_o = \begin{bmatrix} 1 & 0 \\ 0 & 1 \end{bmatrix} \vec{x}_o, \quad (31)$$

where  $u_o := q_m$  is the measured position, and  $\vec{y}_o = [\hat{q}, \dot{\hat{q}}]^T$  are observed position and velocity. The gains designed by

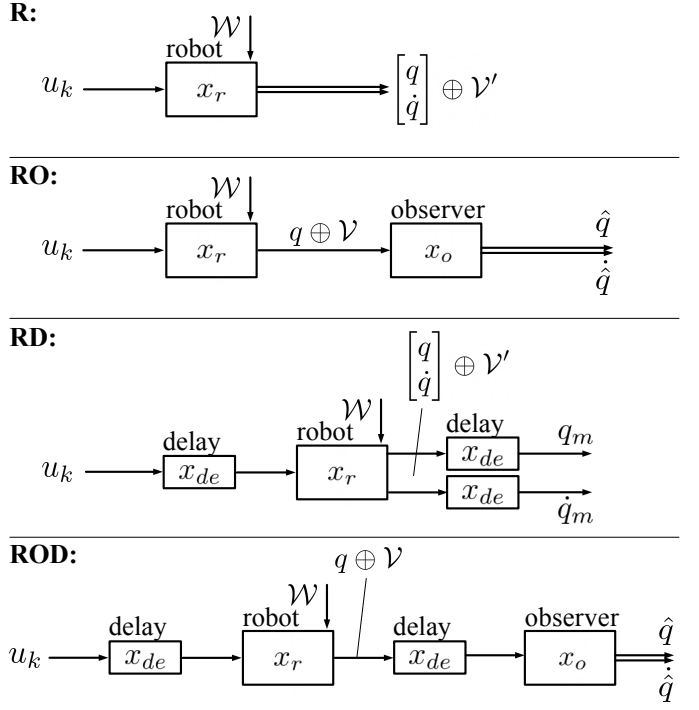


Fig. 3. *Robot model candidates*: Block interconnection diagrams of the model structures and their system states  $x_*$

selecting  $\tilde{h}_1, \tilde{h}_2$  and an  $\epsilon$ , such that  $h_1 := \tilde{h}_1/\epsilon, h_2 := \tilde{h}_2/\epsilon^2$ . On our centralized controller, we implement the discrete-time version from [77].

d) *Delay*: The amount of time delay can seldomly be estimated exactly, and is often time-varying [78]. We assume a delay of one sampling time in each direction: due to synchronization in the fieldbus communication, a computed control signal needs to wait until the next instant for it to be sent. Vice versa, a position measurement is almost retrieved instantly, but has to wait for the next cycle to be sent back to the central controller. Delay is best expressed in discrete-time:

$$\begin{aligned} x_{de}[k+1] &= u_{de}[k], \\ y_{de}[k] &= x_{de}[k], \end{aligned}$$

where  $u_{de}$  is the input signal, and  $y_{de}$  is the signal delayed by one sampling instant. The Pade approximation is a continuous-time model for any time delay [79].

Given the subsystems introduced in the previous paragraphs, we are offered multiple options to choose plant model candidates; an optimal choice is often not immediately clear. Depending on the desired order, we can omit certain subsystems, or decide between a continuous-time or discrete-time version. In this case study, we regard six different plant model candidates with increasing order:

**R-** Only robot dynamics (continuous-time)

**R+** Only robot dynamics (discrete-time)

**RO-** Robot dynamics with observer (continuous)

**RO+** Robot dynamics with observer (discrete)

**RD+** Robot dynamics with delay (discrete)

**ROD+** Robot dynamics with observer and delay (discrete)

TABLE I  
OPEN-LOOP IDENTIFICATION RESULTS: COST (LEMMA 2)

| Model | Axis 1 | Axis 2 | Axis 3 | Axis 4 | Axis 5 | Axis 6 |
|-------|--------|--------|--------|--------|--------|--------|
| R-    | 0.0322 | 0.0422 | 0.0325 | 0.0309 | 0.0505 | 0.0405 |
| R+    | 0.0322 | 0.0422 | 0.0325 | 0.0309 | 0.0505 | 0.0405 |
| RO-   | 0.0033 | 0.0046 | 0.0023 | 0.0028 | 0.0035 | 0.0054 |
| RO+   | 0.0032 | 0.0046 | 0.0022 | 0.0026 | 0.0035 | 0.0053 |
| RD+   | 0.0025 | 0.0044 | 0.0022 | 0.0023 | 0.0035 | 0.0050 |
| ROD+  | 0.0022 | 0.0041 | 0.0021 | 0.0023 | 0.0032 | 0.0041 |

The block interconnection diagram of the models are shown in Fig. 3. All candidates have the same inputs and outputs, such that we can use the same dataset to identify all models. For candidates that omit the observer we apply an alternative measurement error  $\mathcal{V}' \in \mathbb{R}^2$  to satisfy Lemma 4. Since all the candidates are series interconnections of linear subsystems, their respective composition are also linear.

Initially, we evaluate the quality of the model candidates by comparing the cost (11) of the open-loop identification of the unknown disturbances  $\mathcal{W}, \mathcal{V}$ . To make the comparison concise, we assume zonotopes  $\mathcal{W} := (0, G'_W \text{diag}(\vec{\alpha}_W))$  and  $\mathcal{V} := (0, G'_V \text{diag}(\vec{\alpha}_V))$  for all models, where  $G_W = I$  and  $G_V = I$  are fixed. The parameter set thus only consists of  $\mathcal{P} = \{\alpha_W, \alpha_V\}$ , so that the identification problem is a linear program and can be solved using Theorem 1. The initial dataset for this and all subsequent synthesis problems has been obtained from the real robot running trapezoidal and polynomial trajectories with random target positions, velocities, and accelerations<sup>1</sup>. The initial gains for the state-feedback controller and linear observer have been manually tuned to  $\omega = 20$ ,  $\zeta = 0.65$ ,  $\bar{h}_1 = 15$ ,  $\bar{h}_2 = 30$ ,  $\epsilon = 0.01$ . An automatic preselection was done to avoid trajectories that lead to self-collision or exceeding the maximum motor currents. The total duration of the initial dataset is 33 minutes and 20 seconds. We maximize the number of test cases by considering each sampling instant as a starting point of a new test case, resulting in 497,880 test cases for each joint. The initial states  $x[0]$  for each model and test case can be mostly derived from the measurements and by tracking the corresponding signals on our controller. Only for the initial robot velocities, we choose to use offline zero-phase-filtering [80], because it resulted in smaller identified disturbances compared to using the observed velocity, which ultimately, according to (19), means that the offline method delivers a better velocity estimation. The resulting costs are shown in Tab. I, and the corresponding parameters are shown in Tab. II.

The open-loop identification results clearly show that the cost decreases with increasing model order for every robot axis. A decrease is also visible for  $\alpha_{W,2}$ , which corresponds to the size of non-determinism of the robot acceleration. A significant difference between discrete-time and continuous-time model candidates in terms of cost is not visible. The computation time for all models are within seconds, when using MATLAB, irregardless of the model order. This evaluation indicates that the ROD+ model is the best model candidate

<sup>1</sup>A video showing the initial tests, and the code for reproducing all experiments are provided within the supplementary materials.

TABLE II  
OPEN-LOOP IDENTIFICATION RESULTS: NON-DETERMINISMS OF AXIS 1

| Model | $\alpha_{W,1}$ | $\alpha_{W,2}$ | $\alpha_{V,1}$ | $\alpha_{V,2}$ |
|-------|----------------|----------------|----------------|----------------|
| R-    | 0.0184         | 2.2009         | 0.0001         | 0.0298         |
| R+    | 0.0184         | 2.2009         | 0.0001         | 0.0298         |
| RO-   | 0.0386         | 1.4494         | 0.0000         | —              |
| RO+   | 0.0401         | 1.7321         | 0              | —              |
| RD+   | 0.0127         | 1.7762         | 0.0001         | 0.0207         |
| ROD+  | 0.0434         | 0.7556         | 0              | —              |

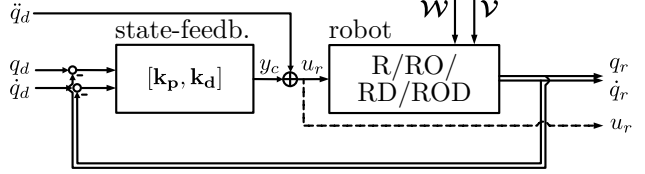


Fig. 4. Simultaneous state-feedback synthesis and identification: we minimize  $\mathcal{R}_{q_r, \dot{q}_r}$  and  $\mathcal{R}_{u_r}$  is under constraint. Variables are shown in **bold**.

with the smallest reachable set and least amount of non-determinism.

### B. State-feedback control synthesis

In this section of our case study, we apply our iterative synthesis approach from Sec. III-D to the problem of designing the state-feedback controller in (29). The feedback-linearization, which decouples the dynamics of robot joints, is a major simplification, since it allows us to synthesize the controller for each joint separately. The synthesis goal is to reduce the reachable set of the tracking error taking into account the limited motor capabilities, while simultaneously identifying reachset conforming disturbances of the robot. We evaluate the same model candidates as in the previous experiment. The block diagram of the closed-loop system is shown in Fig. 4. The reference for each axis is the desired trajectory  $\vec{y}_{\text{ref}} := [q_d, \dot{q}_d]^T$  and  $u_{\text{ref}} = \dot{q}_d$ , the outputs of the closed-loop system are  $\vec{y}_z = \vec{y}_p$  and  $\vec{y}_{\text{con}} = u_r$ , where  $\vec{y}_p$  consists of the output position and velocity of the robot (see Fig. 3), and  $u_r$  is the plant input.

The synthesis goal is to reduce the position and velocity error of the terminal reachable set:

$$\begin{aligned} \min_{\mathcal{P}} \quad & \|\mathcal{R}_{q_r, \dot{q}_r}(t_\infty)\|, \\ \text{subject to} \quad & (13), \\ & \forall t: \mathcal{R}_{\text{con}}(t) \subseteq \mathcal{Y}_c, \end{aligned}$$

and

$$\mathcal{P} := \{\omega, \zeta, \alpha_W, \alpha_V\}.$$

To find the appropriate  $\mathcal{Y}_c$ , according to (24), we reserve  $\ddot{q}_d \in \mathcal{U}_{\text{ref}} = [-3, 3] \text{ m/s}^2$ . We then derive, for each axis  $i$ , the upper limit of the input  $u_r \in \mathcal{U}_{p,i}$  from the peak torques of the motors, which are  $\vec{\tau}_{\text{max}} = [75.5, 75.5, 75.5, 75.5, 20, 20]^T \text{ Nm}$ . We fit the largest intervals for  $\mathcal{U}_{p,i}$  of each joint that adheres to  $\vec{\tau} \leq \vec{\tau}_{\text{max}}$  by evaluating (28) with  $\vec{u} := \mathcal{U}_{p,1} \times \dots \times \mathcal{U}_{p,6}$  and randomly sampled  $q, \dot{q}$ . We determined that  $\mathcal{U}_{p,2} = [-7.27, 7.27] \text{ rad/s}^2$ , for axis 2, and  $\mathcal{U}_{p,i} = [-20, 20]$ , for all

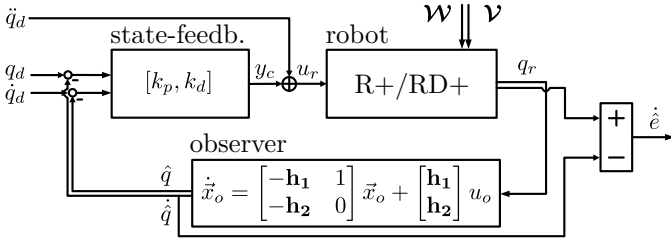


Fig. 5. Simultaneous observer synthesis and identification (Approach 1): we minimize  $\mathcal{R}_{\dot{e}}$ . Variables are shown in **bold**.

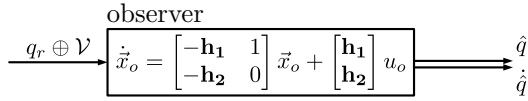


Fig. 6. Observer synthesis (Approach 2): we minimize the transient duration of a set of step responses. Variables are shown in **bold**.

other axes, are admissible intervals. Thus, by applying (24),  $\mathcal{Y}_c = [-4.27, 4.27]$  for axis 2 and  $\mathcal{Y}_c = [-17, 17]$  for the other axes. The iterative synthesis is performed for each axis individually. The initial dataset for the first iteration is the same as in the open-loop identification. For subsequent iterations, we run a validation trajectory to obtain new data. The results of the synthesis is shown in Tab. III.

The ROD+ model is the only one, that converges after one iteration, meaning that when running the validation trajectory with the optimized values, the robot did not produce new data, for which the identified model was not reachset conformant. We can see that the R and RO models are not suitable for controller synthesis: the first iteration produced control gains, that were too high, and for which the real robot became unstable. Thus, the second iteration did not yield feasible solutions, since the identified non-determinism were too large. Only RD+ and ROD+ produced converging solutions, because they modelled the delay dynamics. This helped the reachability analysis to predict the instability, when using high gains, because the reachable sets would grow very large, thus letting the optimization avoid them.

### C. Observer synthesis

We study the problem of designing the linear observer in (30). In this paper, we propose two different reachability-based approaches than can be realized within our framework.

- **Approach 1:** we minimize velocity estimation error, considering the closed-loop system as depicted in Fig. 5. We obtain an invariant set, towards which the reachable maximal velocity estimation error converges.
- **Approach 2:** given a set of step responses, we minimize the duration of the transient, as well as the reachable steady-state error of the observer system. This approach is inspired by the works in [81], where the authors formally proved the boundedness of high-gain observers with measurement errors.

Like the state-feedback example, we formulate Approach 1 for each joint as an iterative synthesis problem (Sec. III-D),

since it involves identifying the robot plant. Approach 2 only analyses the known observer system, so that the reachability-based control synthesis method of Sec. III-C is sufficient.

*Approach 1:* The reference input and output are the same as for the state-feedback example:  $\vec{y}_{\text{ref}} := [q_d, \dot{q}_d]^T$ , and  $u_{\text{ref}} = \dot{q}_d$ . The output of the closed-loop system is the estimation error  $y_z = \hat{e} = \dot{q} - \dot{q}_d$ . Notice, that because the unmeasurable 'true' velocity  $\dot{q}$  of the robot system is analysed here, we need to include an estimation (e.g., using an observed value) within the test data for the identification. This does not conflict with the synthesis, because the test data is only relevant for identification, while Approach 1 optimizes the resulting dynamics from a new observer. For brevity, we omit the input constraints. The overall synthesis is formalized in the following optimization problem:

$$\begin{aligned} \min_{\mathcal{P}} \quad & \|\mathcal{R}_{\dot{e}}(t_{\infty})\|, \\ \text{subject to} \quad & (13), \end{aligned}$$

and

$$\mathcal{P} := \{\tilde{h}_1, \tilde{h}_2, \alpha_W, \alpha_V\},$$

where  $\mathcal{R}_{\dot{e}}(t_{\infty})$  is a positively invariant set, towards which the velocity estimation error converges. Since  $\epsilon$  is a redundant parameter, we fix it at  $\epsilon = 0.01$ . Like in the state-feedback synthesis, we optimize the scaling parameters  $\alpha_W, \alpha_V$  of the robot non-determinism. Since the observer is implemented in discrete-time, we only consider the discrete-time robot model candidates R+ and RD+. The results of the synthesis is shown in Tab. IV.

The iterative synthesis converged after one iteration for both model candidates. In contrast to the open-loop identification and state-feedback synthesis, we see that the R+ model lead to the smallest final reachable set. Despite the varying non-determinisms of the robot, the optimal observer parameters are very similar across all axes, which indicates that  $\mathcal{W}, \mathcal{V}$  do not influence the observer dynamics much, but affect the final reachable set.

*Approach 2:* The goal of the synthesis is to minimize the transient response time, as well as the steady-state error caused by the measurement error. As [81] points out, these are conflicting goals for high-gain observers, because a faster transient leads to noise amplification, while a slower transient attenuates noise. To resolve this conflict, we consider the transient response time as the sole cost, while we regard the maximum steady-state error as an constraint. The overall synthesis is formalized in the following optimization problem:

$$\begin{aligned} \min_{\mathcal{P}} \quad & t_{\infty}, \\ \text{subject to} \quad & \mathcal{R}_{\dot{q}, \dot{q}}(t_{\infty}) \in \mathcal{Y}_s, \end{aligned}$$

and

$$\mathcal{P} := \{\tilde{h}_1, \tilde{h}_2\},$$

where  $\mathcal{R}_{\dot{q}, \dot{q}}(t_{\infty})$  is the positive invariant set representing the steady-state error, towards which the system converges, and  $t_{\infty}$  is the time of the convergence, which we consider as the transient response time. We set the measurement error at  $\mathcal{V} =$

TABLE III  
STATE FEEDBACK CONTROL SYNTHESIS RESULTS FOR ALL CANDIDATE MODELS

| Model | Ax. | Iteration 1 |              |             |                |                |                | Iteration 2    |      |              |         |                |                |      |
|-------|-----|-------------|--------------|-------------|----------------|----------------|----------------|----------------|------|--------------|---------|----------------|----------------|------|
|       |     | cost        | $\omega$     | $\zeta$     | $\alpha_{W,1}$ | $\alpha_{W,2}$ | $\alpha_{V,1}$ | $\alpha_{V,2}$ | cost | $\omega$     | $\zeta$ | $\alpha_{W,1}$ | $\alpha_{W,2}$ |      |
| R-    | 1   | 0.16        | 100.00       | 0.90        | 0.00           | 2.15           | 0.00           | 0.02           | *    | *            | *       | *              | *              | *    |
|       | 2   | 1.07        | 7.12         | 0.74        | 0.00           | 2.05           | 0.00           | 0.09           | *    | *            | *       | *              | *              | *    |
|       | 3   | 0.22        | 100.00       | 0.76        | 0.00           | 1.50           | 0.00           | 0.04           | *    | *            | *       | *              | *              | *    |
|       | 4   | 0.22        | 97.05        | 0.80        | 0.00           | 2.85           | 0.00           | 0.03           | *    | *            | *       | *              | *              | *    |
|       | 5   | 0.28        | 78.81        | 0.75        | 0.00           | 3.23           | 0.00           | 0.04           | *    | *            | *       | *              | *              | *    |
|       | 6   | 0.43        | 47.75        | 0.86        | 0.00           | 4.93           | 0.00           | 0.05           | *    | *            | *       | *              | *              | *    |
| R+    | 1   | 0.21        | 98.29        | 1.00        | 0.01           | 2.25           | 0.00           | 0.02           | *    | *            | *       | *              | *              | *    |
|       | 2   | 1.77        | 3.81         | 1.00        | 0.06           | 2.05           | 0.00           | 0.09           | *    | *            | *       | *              | *              | *    |
|       | 3   | 0.30        | 75.71        | 0.85        | 0.03           | 1.54           | 0.00           | 0.04           | *    | *            | *       | *              | *              | *    |
|       | 4   | 0.30        | 73.75        | 0.89        | 0.02           | 3.01           | 0.00           | 0.03           | *    | *            | *       | *              | *              | *    |
|       | 5   | 0.36        | 61.44        | 0.88        | 0.02           | 3.32           | 0.00           | 0.04           | *    | *            | *       | *              | *              | *    |
|       | 6   | 0.49        | 43.78        | 0.91        | 0.01           | 5.02           | 0.00           | 0.05           | *    | *            | *       | *              | *              | *    |
| RO-   | 1   | <i>0.24</i> | <i>21.18</i> | <i>1.00</i> | <i>0.05</i>    | <i>0.00</i>    | <i>0.00</i>    | —              | —    | —            | —       | —              | —              | —    |
|       | 2   | 0.27        | <i>16.31</i> | <i>1.00</i> | <i>0.05</i>    | <i>0.00</i>    | <i>0.00</i>    | —              | —    | —            | —       | —              | —              | —    |
|       | 3   | 0.18        | 42.16        | 1.00        | 0.04           | 0.00           | 0.00           | —              | *    | *            | *       | *              | *              | *    |
|       | 4   | 0.12        | 40.02        | 1.00        | 0.02           | 0.00           | 0.00           | —              | *    | *            | *       | *              | *              | —    |
|       | 5   | 0.18        | 42.48        | 1.00        | 0.04           | 0.00           | 0.00           | —              | *    | *            | *       | *              | *              | —    |
|       | 6   | 0.21        | 43.83        | 1.00        | 0.04           | 0.00           | 0.00           | —              | *    | *            | *       | *              | *              | —    |
| RO+   | 1   | 0.29        | 40.03        | 1.00        | 0.03           | 1.63           | 0.00           | —              | *    | *            | *       | *              | *              | —    |
|       | 2   | <i>1.22</i> | <i>4.73</i>  | <i>1.00</i> | <i>0.09</i>    | <i>1.91</i>    | <i>0.00</i>    | —              | —    | —            | —       | —              | —              | —    |
|       | 3   | 0.30        | 37.83        | 1.00        | 0.03           | 1.33           | 0.00           | —              | *    | *            | *       | *              | *              | —    |
|       | 4   | 0.35        | 46.69        | 1.00        | 0.04           | 2.48           | 0.00           | —              | *    | *            | *       | *              | *              | —    |
|       | 5   | 0.35        | 47.97        | 1.00        | 0.03           | 3.44           | 0.00           | —              | *    | *            | *       | *              | *              | —    |
|       | 6   | 0.48        | 38.31        | 1.00        | 0.04           | 4.52           | 0.00           | —              | *    | *            | *       | *              | *              | —    |
| RD+   | 1   | <b>0.31</b> | <i>35.46</i> | 0.79        | 0.02           | <i>1.88</i>    | 0.00           | 0.02           | —    | —            | —       | —              | —              | —    |
|       | 2   | <i>1.74</i> | <i>3.96</i>  | <i>1.00</i> | <i>0.08</i>    | <i>1.99</i>    | <i>0.00</i>    | <i>0.08</i>    | —    | —            | —       | —              | —              | —    |
|       | 3   | <i>0.38</i> | <i>29.65</i> | <i>0.80</i> | <i>0.03</i>    | <i>1.38</i>    | <i>0.00</i>    | <i>0.03</i>    | —    | —            | —       | —              | —              | —    |
|       | 4   | <b>0.42</b> | <i>35.48</i> | 0.79        | 0.03           | <i>2.61</i>    | 0.00           | 0.03           | —    | —            | —       | —              | —              | —    |
|       | 5   | 0.51        | 35.48        | 0.79        | 0.03           | 3.17           | 0.00           | 0.03           | 0.56 | <i>38.24</i> | 0.85    | 0.03           | <i>4.08</i>    | 0.00 |
|       | 6   | 0.58        | 36.51        | 0.90        | 0.03           | 4.71           | 0.00           | 0.03           | 0.71 | <i>29.76</i> | 1.00    | 0.02           | 6.59           | 0.00 |
| ROD+  | 1   | <i>0.37</i> | <i>19.28</i> | <i>1.00</i> | <i>0.03</i>    | <i>1.37</i>    | <i>0.00</i>    | —              | —    | —            | —       | —              | —              | —    |
|       | 2   | <b>1.15</b> | <i>4.92</i>  | <i>1.00</i> | <i>0.09</i>    | <i>1.74</i>    | <i>0.00</i>    | —              | —    | —            | —       | —              | —              | —    |
|       | 3   | <b>0.37</b> | <i>18.67</i> | <i>1.00</i> | <i>0.04</i>    | <i>1.18</i>    | <i>0.00</i>    | —              | —    | —            | —       | —              | —              | —    |
|       | 4   | 0.50        | <i>20.85</i> | <i>1.00</i> | <i>0.04</i>    | <i>2.14</i>    | <i>0.00</i>    | —              | —    | —            | —       | —              | —              | —    |
|       | 5   | <b>0.54</b> | <i>19.28</i> | <i>1.00</i> | <i>0.05</i>    | <i>2.09</i>    | <i>0.00</i>    | —              | —    | —            | —       | —              | —              | —    |
|       | 6   | <b>0.67</b> | <i>21.75</i> | <i>1.00</i> | <i>0.04</i>    | <i>3.79</i>    | <i>0.00</i>    | —              | —    | —            | —       | —              | —              | —    |

**bold:** best model candidate for this axis, *italic:* converged values,  $*$ : infeasible solution,  $-$ : not evaluated

TABLE IV  
OBSERVER SYNTHESIS RESULTS (APPROACH 1)

| Model | Ax. | Iteration 1 |               |               |                |                |                |      |
|-------|-----|-------------|---------------|---------------|----------------|----------------|----------------|------|
|       |     | cost        | $\tilde{h}_1$ | $\tilde{h}_2$ | $\alpha_{W,1}$ | $\alpha_{W,2}$ | $\alpha_{V,1}$ |      |
| R+    | 1   | <b>0.12</b> | 10.55         | 29.73         | 0.03           | 1.58           | 0.00           | 0.10 |
|       | 2   | <b>0.16</b> | 11.72         | 45.85         | 0.02           | 5.89           | 0.00           | 0.03 |
|       | 3   | <b>0.13</b> | 10.55         | 29.73         | 0.03           | 1.32           | 0.00           | 0.09 |
|       | 4   | <b>0.15</b> | 10.55         | 29.73         | 0.04           | 2.41           | 0.00           | 0.10 |
|       | 5   | <b>0.14</b> | 10.55         | 29.73         | 0.03           | 3.07           | 0.00           | 0.07 |
|       | 6   | <b>0.20</b> | 10.55         | 29.73         | 0.04           | 4.11           | 0.00           | 0.08 |
| RD+   | 1   | 0.21        | 7.99          | 21.79         | 0.04           | 2.19           | 0.00           | 0.02 |
|       | 2   | 0.39        | 7.99          | 21.81         | 0.06           | 5.68           | 0.00           | 0.05 |
|       | 3   | 0.21        | 7.99          | 21.82         | 0.03           | 2.26           | 0.00           | 0.02 |
|       | 4   | 0.25        | 7.99          | 21.81         | 0.04           | 3.37           | 0.00           | 0.02 |
|       | 5   | 0.29        | 7.99          | 21.81         | 0.04           | 3.77           | 0.00           | 0.03 |
|       | 6   | 0.31        | 7.99          | 21.81         | 0.04           | 4.15           | 0.00           | 0.04 |

**bold:** best model candidate for this axis

$[-1, 1]$  Millidegrees, and consider a set of step responses by starting the reachability analysis of the observer system with a non-empty set  $x(0) \in \mathcal{X}_0 = [-0.1, 0.1] \times [-0.1, 0.1]$ , while keeping the reference signal  $q_r = 0$ . We constrain the steady-state error of  $\dot{q}$  to  $\mathcal{Y}_s = [-0.005, 0.005]$ . We only analyse the

TABLE V  
OBSERVER SYNTHESIS RESULTS (APPROACH 2)

|  | transient response time [s] | $\tilde{h}_1$ | $\tilde{h}_2$ |
|--|-----------------------------|---------------|---------------|
|  |                             | 0.064         | 10.13         |

discrete-time observer, since this is the one that is implemented on the real controller. The results are shown in Tab. V.

Interestingly, the optimal observer gains obtained through Approach 2 are similar to the ones obtained through Approach 1. In addition, we discover that by increasing the gains for discrete-time observers, the transient response time  $t_\infty$  decreases at first, but increases again, because the system starts to oscillate due to discretization effects. Therefore, the  $t_\infty$  in Tab. V is the actual minimum, without violating  $\mathcal{Y}_s$ . We additionally show this behavior in Fig. 7 by varying  $\epsilon$ : for  $\epsilon = 0.02$ , the steady-state error is small, but  $t_\infty = 0.0112$  s is large. For  $\epsilon = 0.01$ , the steady-state error is still small, and  $t_\infty = 0.064$  s is the smallest. For  $\epsilon = 0.005$ , the steady-state error is large, and so is  $t_\infty = 0.128$  s.

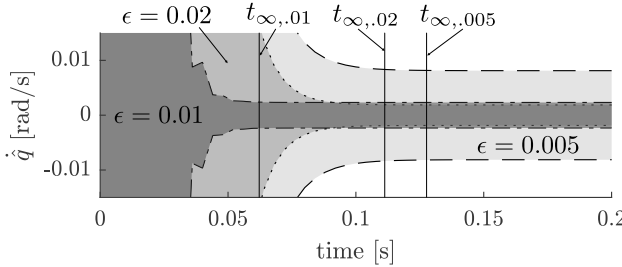


Fig. 7. *Observer synthesis (Approach 2): Comparison of transient response time  $t_\infty$  for  $\epsilon = 0.005, \epsilon = 0.01$ , and  $\epsilon = 0.02$*

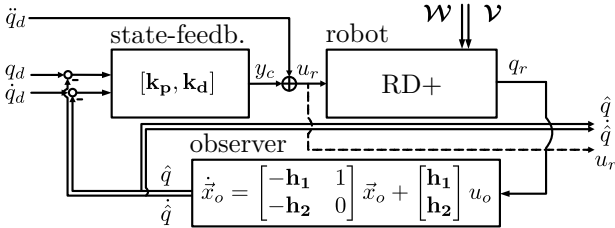


Fig. 8. *Simultaneous output-feedback synthesis and identification: we minimize  $\mathcal{R}_{\dot{q}, \dot{\dot{q}}}$  and  $\mathcal{R}_{u_r}$  is under constraint. Variables are shown in bold.*

#### D. Output-feedback control synthesis

Merging the linear observer and the state-feedback controller, the overall mechanism becomes an output-feedback controller. We briefly show in this section of the case study, that we can also synthesize the controller and observer at the same time. The block diagram is shown in Fig. 8, and the optimization problem is the same one as in Sec. IV-B, except that the parameter set is now  $\mathcal{P} := \{\omega, \zeta, \tilde{h}_1, \tilde{h}_2, \alpha_W, \alpha_V\}$ . For brevity, we only evaluate RD+ as the model candidate the results are shown in Tab. VI.

Because the variable parameter set has now grown, the non-linear programming algorithms often reached local minima. We restarted the synthesis with differing initial values until we reached a global minimum. As we can observe for the cost of each axis, they are all smaller than the corresponding costs of the ROD+ model in Tab. III, for which the reason is obvious: in the previous experiment,  $\tilde{h}_1$  and  $\tilde{h}_2$  were manually tuned and fixed; in this experiment, output-feedback synthesis has found superior values. The observer gains for axis 2 and 6 are significantly larger than the rest, but resulted in smaller reachable sets and did not result in unstable robot behavior.

TABLE VI  
OUTPUT-FEEDBACK SYNTHESIS RESULTS

| Model | Ax. | cost        | $\omega$ | $\zeta$ | Iteration 1   |               |                |                |                |
|-------|-----|-------------|----------|---------|---------------|---------------|----------------|----------------|----------------|
|       |     |             |          |         | $\tilde{h}_1$ | $\tilde{h}_2$ | $\alpha_{W,1}$ | $\alpha_{W,2}$ | $\alpha_{V,1}$ |
| RD+   | 1   | <b>0.37</b> | 18.72    | 1.00    | 11.38         | 27.36         | 0.04           | 1.23           | 0.00           |
|       | 2   | <b>0.85</b> | 6.37     | 1.00    | 59.05         | 37.20         | 0.09           | 1.52           | 0.00           |
|       | 3   | <b>0.37</b> | 18.06    | 1.00    | 10.77         | 25.00         | 0.04           | 1.18           | 0.00           |
|       | 4   | <b>0.48</b> | 20.09    | 1.00    | 11.51         | 27.59         | 0.05           | 1.91           | 0.00           |
|       | 5   | <b>0.48</b> | 17.96    | 1.00    | 11.31         | 27.25         | 0.05           | 1.58           | 0.00           |
|       | 6   | <b>0.64</b> | 22.31    | 1.00    | 119.82        | 360.36        | 0.06           | 3.23           | 0.00           |

#### V. DISCUSSION & CONCLUSION

In the case study, we have shown that reachability-based controller synthesis, together with identification, can be a powerful tool to do formal analysis of various control problems in robotics. We are able to make guarantees on the error of tracking controllers, the estimation errors of observers, and compute optimal output-feedback controllers minimizing these errors.

The performance of the synthesis greatly depend on the models, that have been chosen for the robot. As we examined in the case study, one should model behaviors, that are relevant to the synthesis problem, such as delay and observer dynamics. Finding these, however, requires application-related experience. The rewards for accurate modeling are smaller identified non-determinisms, such that more feasible solutions can be found, and a faster convergence of the iterative synthesis approach. The number of iterations also depend on the initial dataset. If only a low amount of data is provided in the beginning, it is much more likely to find non-conforming behavior in the subsequent iterations.

We provide a general formulation of the reachability-based identification and controller synthesis problem, and present a computationally efficient solution for linear systems. We especially make use of the superposition principle to reduce the amount of set inclusion checks and to analyse the tracking error independently from any reference trajectory. The extension to nonlinear, and hybrid systems is challenging, since the superposition does generally not apply for them. We have focused mostly on computing minimal robustly positive invariant sets. Our approach can also be applied to other safe sets, such as the ones shown in [25].

Together with this paper, we provide software tools to replicate the results and to analyze further control problems of linear systems, e.g., other feedback-linearizing controllers of robots. The compositional framework also makes it easy to analyse networked linear systems. In the future, we plan to implement visual tools, such that an identification and synthesis problem can be directly derived and solved from block diagrams descriptions of the system.

#### ACKNOWLEDGMENT

The authors gratefully acknowledge financial support by the Central Innovation Programme ZF4086004LP7 of the German Federal Government.

#### REFERENCES

- [1] H. Kress-Gazit, M. Lahijanian, and V. Raman, "Synthesis for Robots: Guarantees and Feedback for Robot Behavior," *Annual Review of Control, Robotics, and Autonomous Systems*, vol. 1, no. 1, pp. 211–236, 2018.
- [2] M. Althoff, "An Introduction to CORA 2015 (Tool Presentation)," in *Proc. of the Workshop on Applied Verification for Continuous and Hybrid Systems*, 2015, pp. 120–151.
- [3] P. M. Van Den Hof and R. J. Schrama, "Identification and control - Closed-loop issues," *Automatica*, vol. 31, no. 12, pp. 1751–1770, 1995.
- [4] C. G. Atkeson, C. H. An, and J. M. Hollerbach, "Estimation of Inertial Parameters of Manipulator Loads and Links," *The International Journal of Robotics Research*, vol. 5, no. 3, pp. 101–119, 1986.
- [5] L. Ljung, *System Identification. Theory for the User*, 2nd ed. New Jersey: Prentice Hall, 1999.

- [6] C. H. An, C. G. Atkeson, and J. M. Hollerbach, *Model-based control of a robot manipulator*. MIT press, 1988.
- [7] C. Abdallah, D. M. Dawson, P. Dorato, and M. Jamshidi, “Survey of robust control for rigid robots,” *IEEE Control Systems*, vol. 11, no. 2, pp. 24–30, feb 1991.
- [8] J. Swevers, C. Ganseman, and D. B. T, “Optimal Robot Excitation and Identification.pdf,” vol. 13, no. 5, pp. 730–740, 1997.
- [9] N. Ramdani and P. Poignet, “Robust dynamic experimental identification of robots with set membership uncertainty,” *IEEE/ASME Transactions on Mechatronics*, vol. 10, no. 2, pp. 253–256, 2005.
- [10] R. E. Skelton, “Model error concepts in control design,” *International Journal of Control*, vol. 49, no. 5, pp. 1725–1753, 1989.
- [11] S. G. Douma and P. M. Van Den Hof, “Relations between uncertainty structures in identification for robust control,” *Automatica*, vol. 41, no. 3, pp. 439–457, 2005.
- [12] J. Santolaria and M. Ginés, “Uncertainty estimation in robot kinematic calibration,” *Robotics and Computer-Integrated Manufacturing*, vol. 29, no. 2, pp. 370–384, 2013.
- [13] A. Vicino and G. Zappa, “Sequential approximation of feasible parameter sets for identification with set membership uncertainty,” *IEEE Transactions on Automatic Control*, vol. 41, no. 6, pp. 774–785, jun 1996.
- [14] M. Milanese and C. Novara, “Set Membership identification of nonlinear systems,” *Automatica*, vol. 40, no. 6, pp. 957–975, 2004.
- [15] M. Kieffer, E. Walter, and I. Simeonov, “Guaranteed nonlinear parameter estimation for continuous-time dynamical models,” *Robust Control Design*, vol. 5, pp. 685–690, 2006.
- [16] J. Bravo, T. Alamo, and E. Camacho, “Bounded error identification of systems with time-varying parameters,” *IEEE Transactions on Automatic Control*, vol. 51, no. 7, pp. 1144–1150, jul 2006.
- [17] S. Zhang, L. Dai, Y. Gao, and Y. Xia, “Adaptive interpolating control for constrained systems with parametric uncertainty and disturbances,” *International Journal of Robust and Nonlinear Control*, vol. 30, no. 16, pp. 6838–6852, 2020.
- [18] V. Reppa and A. Tzes, “Fault detection based on orthotopic set membership identification for robot manipulators,” *IFAC Proceedings Volumes (IFAC-PapersOnline)*, vol. 17, no. 1 PART 1, pp. 7344–7349, 2008.
- [19] H. Roehm, J. Oehlerking, M. Woehrle, and M. Althoff, “Model Conformance for Cyber-Physical Systems,” *ACM Transactions on Cyber-Physical Systems*, vol. 3, no. 3, pp. 1–26, aug 2019.
- [20] Y. Chen, H. Peng, J. Grizzle, and N. Ozay, “Data-Driven Computation of Minimal Robust Control Invariant Set,” *Proceedings of the IEEE Conference on Decision and Control*, vol. 2018–December, no. Cdc, pp. 4052–4058, 2019.
- [21] S. Sadraddini and C. Belta, “Formal guarantees in data-driven model identification and control synthesis,” *HSCC 2018 - Proceedings of the 21st International Conference on Hybrid Systems: Computation and Control (part of CPS Week)*, pp. 147–156, 2018.
- [22] B. Schurmann, D. Heß, J. Eilbrecht, O. Stursberg, F. Köster, and M. Althoff, “Ensuring drivability of planned motions using formal methods,” *IEEE Conference on Intelligent Transportation Systems, Proceedings, ITSC*, vol. 2018–March, pp. 1–8, 2018.
- [23] M. Althoff and J. M. Dolan, “Reachability computation of low-order models for the safety verification of high-order road vehicle models,” in *American Control Conference (ACC)*, 2012, pp. 3559–3566.
- [24] Z. Wang and R. M. Jungers, “Scenario-Based Set Invariance Verification for Black-Box Nonlinear Systems,” *IEEE Control Systems Letters*, vol. 5, no. 1, pp. 193–198, 2021.
- [25] F. Gruber and M. Althoff, “Computing Safe Sets of Linear Sampled-Data Systems,” *IEEE Control Systems Letters*, vol. 5, no. 2, pp. 1–1, 2020.
- [26] M. Althoff, A. Giusti, S. B. Liu, and A. Pereira, “Effortless creation of safe robots from modules through self-programming and self-verification,” *Science Robotics*, vol. 4, no. 31, p. eaaw1924, jun 2019.
- [27] S. B. Liu and M. Althoff, “Reachset Conformance of Forward Dynamic Models for the Formal Analysis of Robots,” in *2018 IEEE/RSJ International Conference on Intelligent Robots and Systems (IROS)*. IEEE, oct 2018, pp. 370–376. [Online]. Available: <https://ieeexplore.ieee.org/document/8593975/>
- [28] A. Giusti, S. B. Liu, and M. Althoff, “Interval-Arithmetic-Based Robust Control of Fully-Actuated Mechanical Systems,” *IEEE Transactions on Control Systems Technology*, vol. XX, no. X, pp. 1–12, 2021.
- [29] T. Dang, T. Dreossi, E. Fanchon, O. Maler, C. Piazza, and A. Rocca, *Set-Based Analysis for Biological Modeling*. Springer International Publishing, 2019.
- [30] G. Batt, C. Belta, and R. Weiss, “Model checking genetic regulatory networks with parameter uncertainty,” *Lecture Notes in Computer Science (including subseries Lecture Notes in Artificial Intelligence and Lecture Notes in Bioinformatics)*, vol. 4416 LNCS, pp. 61–75, 2007.
- [31] M. Kloetzer and C. Belta, “A fully automated framework for control of linear systems from temporal logic specifications,” *IEEE Transactions on Automatic Control*, vol. 53, no. 1, pp. 287–297, 2008.
- [32] M. Zamani, G. Pola, M. Mazo Jr., and P. Tabuada, “Symbolic models for nonlinear control systems without stability assumptions,” *IEEE Transactions on Automatic Control*, vol. 57, no. 7, pp. 1804–1809, 2012.
- [33] J. A. DeCastro and H. Kress-Gazit, “Synthesis of nonlinear continuous controllers for verifiably correct high-level, reactive behaviors,” *The International Journal of Robotics Research*, vol. 34, no. 3, pp. 378–394, 2015.
- [34] G. E. Fainekos, A. Girard, H. Kress-Gazit, and G. J. Pappas, “Temporal logic motion planning for dynamic robots,” *Automatica*, vol. 45, no. 2, pp. 343–352, 2009.
- [35] A. Girard, “Controller synthesis for safety and reachability via approximate bisimulation,” *Automatica*, vol. 48, no. 5, pp. 947–953, 2012.
- [36] H. Kress-Gazit, G. E. Fainekos, and G. J. Pappas, “Temporal-logic-based reactive mission and motion planning,” *Transactions on Robotics*, vol. 25, no. 6, pp. 1370–1381, 2009.
- [37] J. Liu, N. Ozay, U. Topcu, and R. M. Murray, “Synthesis of reactive switching protocols from temporal logic specifications,” *IEEE Transactions on Automatic Control*, vol. 58, no. 7, pp. 1771–1785, 2013.
- [38] J. Liu and N. Ozay, “Finite abstractions with robustness margins for temporal logic-based control synthesis,” *Nonlinear Analysis: Hybrid Systems*, vol. 22, pp. 1 – 15, 2016.
- [39] G. Pola, A. Girard, and P. Tabuada, “Symbolic models for nonlinear control systems using approximate bisimulation,” in *Proc. of the 46th Conference on Decision and Control*, 2007, pp. 4656–4661.
- [40] V. Raman, A. Donzé, D. Sadigh, R. M. Murray, and S. A. Seshia, “Reactive synthesis from signal temporal logic specifications,” in *Proceedings of the 18th International Conference on Hybrid Systems: Computation and Control*, 2015, pp. 239–248.
- [41] M. Rungger, M. Mazo Jr., and P. Tabuada, “Specification-guided controller synthesis for linear systems and safe linear-time temporal logic,” in *Proceedings of the 16th International Conference on Hybrid Systems: Computation and Control*. ACM, 2013, pp. 333–342.
- [42] M. Zamani, A. Abate, and A. Girard, “Symbolic models for stochastic switched systems: A discretization and a discretization-free approach,” *Automatica*, vol. 55, pp. 183–196, 2015.
- [43] E. M. Wolff and R. M. Murray, “Optimal control of nonlinear systems with temporal logic specifications,” in *Robotics Research*. Springer, 2016, pp. 21–37.
- [44] J. A. DeCastro and H. Kress-Gazit, “Nonlinear controller synthesis and automatic workspace partitioning for reactive high-level behaviors,” in *Proc. of Hybrid Systems: Computation and Control*, 2016.
- [45] I. Saha, R. Ramaithitima, V. Kumar, G. J. Pappas, and S. A. Seshia, “Automated composition of motion primitives for multi-robot systems from safe LTL specifications,” in *Proc. of the International Conference on Intelligent Robots and Systems*, 2014, pp. 1525–1532.
- [46] R. G. Sanfelice and E. Frazzoli, “A hybrid control framework for robust maneuver-based motion planning,” in *Proc. of the American Control Conference*, 2008, pp. 2254–2259.
- [47] R. Tedrake, I. R. Manchester, M. Tobenkin, and J. W. Roberts, “LQR-trees: Feedback motion planning via sums-of-squares verification,” *The International Journal of Robotics Research*, vol. 29, no. 8, pp. 1038–1052, 2010.
- [48] A. Majumdar and R. Tedrake, “Funnel libraries for real-time robust feedback motion planning,” *The International Journal of Robotics Research*, vol. 36, no. 8, pp. 947–982, 2017.
- [49] B. Schürmann and M. Althoff, “Convex interpolation control with formal guarantees for disturbed and constrained nonlinear systems,” in *Proc. of the International Conference on Hybrid Systems: Computation and Control*, 2017, pp. 121–130.
- [50] —, “Guaranteeing constraints of disturbed nonlinear systems using set-based optimal control in generator space,” in *Proc. of the 20th IFAC World Congress*, 2017, pp. 12 020–12 027.
- [51] —, “Optimal control of sets of solutions to formally guarantee constraints of disturbed linear systems,” in *Proc. of the American Control Conference*, 2017, pp. 2522–2529.
- [52] D. Q. Mayne, M. M. Seron, and S. V. Raković, “Robust model predictive control of constrained linear systems with bounded disturbances,” *Automatica*, vol. 41, no. 2, pp. 219 – 224, 2005.

[53] W. Langson, I. Chryssochoos, S. Raković, and D. Mayne, "Robust model predictive control using tubes," *Automatica*, vol. 40, no. 1, pp. 125 – 133, 2004.

[54] S. V. Raković, B. Kouvaritakis, M. Cannon, C. Panos, and R. Findeisen, "Parameterized tube model predictive control," *IEEE Transactions on Automatic Control*, vol. 57, no. 11, pp. 2746–2761, 2012.

[55] S. V. Raković, B. Kouvaritakis, R. Findeisen, and M. Cannon, "Homothetic tube model predictive control," *Automatica*, vol. 48, no. 8, pp. 1631–1638, 2012.

[56] M. Rubagotti, D. M. Raimondo, A. Ferrara, and L. Magni, "Robust model predictive control with integral sliding mode in continuous-time sampled-data nonlinear systems," *IEEE Transactions on Automatic Control*, vol. 56, no. 3, pp. 556–570, 2011.

[57] L. Magni, G. De Nicolao, R. Scattolini, and F. Allgöwer, "Robust model predictive control for nonlinear discrete-time systems," *International Journal of Robust and Nonlinear Control*, vol. 13, no. 3-4, pp. 229–246, 2003.

[58] D. Q. Mayne, E. C. Kerrigan, E. J. van Wyk, and P. Falugi, "Tube-based robust nonlinear model predictive control," *International Journal of Robust and Nonlinear Control*, vol. 21, no. 11, pp. 1341–1353, 2011.

[59] S. Singh, A. Majumdar, J.-J. Slotine, and M. Pavone, "Robust online motion planning via contraction theory and convex optimization," in *Proc. of the IEEE International Conference on Robotics and Automation*, 2017, pp. 5883–5890.

[60] J. Wolff and M. Buss, "Invariance control design for constrained nonlinear systems," *IFAC Proceedings Volumes*, vol. 38, no. 1, pp. 37 – 42, 2005, 16th IFAC World Congress.

[61] M. Kimmel and S. Hirche, "Invariance control with chattering reduction," in *Proc. of the 53rd Conference on Decision and Control*. IEEE, 2014, pp. 68–74.

[62] A. D. Ames, X. Xu, J. W. Grizzle, and P. Tabuada, "Control barrier function based quadratic programs for safety critical systems," *IEEE Transactions on Automatic Control*, vol. 62, no. 8, pp. 3861–3876, 2016.

[63] P. Wieland and F. Allgöwer, "Constructive safety using control barrier functions," *IFAC Proceedings Volumes*, vol. 40, no. 12, pp. 462–467, 2007.

[64] H. G. Sage, M. F. De Mathelin, and E. Ostertag, "Robust control of robot manipulators: A survey," *International Journal of Control*, vol. 72, no. 16, pp. 1498–1522, 1999.

[65] B. Siciliano, L. Sciavicco, L. Villani, and G. Oriolo, *Robotics*, ser. Advanced Textbooks in Control and Signal Processing. London: Springer London, 2009.

[66] S. Zenieh and M. Corless, "Simple Robust  $r\alpha$  Tracking Controllers for Uncertain Fully-Actuated Mechanical Systems," *Journal of Dynamic Systems, Measurement, and Control*, vol. 119, no. 4, pp. 821–825, dec 1997.

[67] Z. Qu, J. F. Dorsey, X. Zhang, and D. M. Dawson, "Robust control of robots by the computed torque law," *Systems and Control Letters*, vol. 16, no. 1, pp. 25–32, 1991.

[68] M. J. Kim, Y. Choi, and W. K. Chung, "Bringing nonlinear H-infinity optimality to robot controllers," *IEEE Transactions on Robotics*, vol. 31, no. 3, pp. 682–698, 2015.

[69] M. Makarov, M. Grossard, P. Rodríguez-Ayerbe, and D. Dumur, "Modeling and Preview H-infinity Control Design for Motion Control of Elastic-Joint Robots with Uncertainties," *IEEE Transactions on Industrial Electronics*, vol. 63, no. 10, pp. 6429–6438, 2016.

[70] M. Althoff, O. Stursberg, and M. Buss, "Computing reachable sets of hybrid systems using a combination of zonotopes and polytopes," *Nonlinear Analysis: Hybrid Systems*, vol. 4, no. 2, pp. 233–249, may 2010.

[71] M. Althoff, G. Frehse, and A. Girard, "Set Propagation Techniques for Reachability Analysis," pp. 1–27, 2020.

[72] E. L. Duke, "Combining and connecting linear, multi-input, multi-output subsystem models," NASA Technical Memorandum 85912, Edwards, CA, Tech. Rep., 1986.

[73] M. James, "The generalised inverse," *The Mathematical Gazette*, vol. 62, no. 420, pp. 109–114, jun 1978.

[74] B. Schürmann and M. Althoff, "Optimizing sets of solutions for controlling constrained nonlinear systems," 2021, accepted for Publication in IEEE Transactions on Automatic Control.

[75] A. Mohammadi, M. Tavakoli, H. J. Marquez, and F. Hashemzadeh, "Nonlinear disturbance observer design for robotic manipulators," *Control Engineering Practice*, vol. 21, no. 3, pp. 253–267, 2013.

[76] S. Nicosia, A. Tornambè, and P. Valigi, "State estimation in robotic manipulators: Some experimental results," *Journal of Intelligent & Robotic Systems*, vol. 7, no. 3, pp. 321–351, jun 1993.

[77] K. Busawon and H. K. Khalil, "Chapter 9: Digital Implementation," in *High-Gain Observers in Nonlinear Feedback Control*. Philadelphia, PA: Society for Industrial and Applied Mathematics, jun 2017, vol. 0, no. December, pp. 279–311.

[78] Y.-c. Liu and N. Chopra, "Control of Robotic Manipulators Under Input / Output Communication Delays : Theory and Experiments," vol. 28, no. 3, pp. 742–751, 2012.

[79] G. H. Golub and C. F. V. Loan, *Matrix Computations*. Baltimore: Johns Hopkins University Press, 1989.

[80] A. V. Oppenheim, R. W. Schafer, and J. R. Buck, *Discrete-Time signal processing*, 2nd ed. NJ: Prentice Hall, 1999.

[81] A. A. Prasov and H. K. Khalil, "A nonlinear high-gain observer for systems with measurement noise in a feedback control framework," *IEEE Transactions on Automatic Control*, vol. 58, no. 3, pp. 569–580, 2013.